

## Auto-correlation of Binary Stars

S. K. Saha<sup>1</sup> and D. Maitra<sup>2</sup>  
Indian Institute of Astrophysics  
Bangalore 560034  
India

**Abstract:** Speckle interferometric technique is used to record a series of short exposure images of several close binary stars with sub-arcsecond separation through a narrow band filter centred at  $H\alpha$  at the Cassegrain focus of the 2.34 meter (m) Vainu Bappu telescope (VBT), situated at Vainu Bappu Observatory (VBO), Kavalur . The auto-correlation method is developed under Image Reduction Analysis Facility (IRAF). Wiener filter is included in the programme to eliminate spurious high frequency contributions; a few sets of data provide the optimised results. The auto-correlated image of these stars gives the separation of the binary components.

**Keywords:** Speckle Imaging, Auto-correlation, Binary stars, Wiener filter.

**PACS Nos:** 07.60.Ly, 42.30.Wb, 95.55.Br

### 1. Introduction

The speckle interferometric technique [1] is widely used to decode the deleterious effect of the atmospheric turbulence that limits the sensitivity of ground-based telescopes. Recent reviews by Saha [2, 3] describe in depth the utility of this method. One of the important subjects in stellar astrophysics is the studies of close binary stars, that play a fundamental role in measuring stellar masses, providing a benchmark for stellar evolution calculations; a long-term benefit of interferometric imaging is a better calibration of the main-sequence mass-luminosity relationship [4]. The procedure in obtaining masses of stars involves combining the spectroscopic orbit with the astrometric orbit, which is the projection of true orbit on the sky, from the interferometric data [5]. In order to derive accurate orbital elements and masses, luminosities and distances, continuous observations of spectroscopic binaries are essential. Major contributions in resolving close binary systems, among others, came from the Center for High

---

<sup>1</sup>e-mail: sks@iiap.ernet.in

<sup>2</sup>Summer project student from Indian Institute of Technology Kanpur 208016, India

Angular Resolution Astronomy (CHARA) at Georgia State University, USA [6-9]. Survey of visual and interferometric binary stars have also been reported by the other groups [10-19].

Most of these results that appeared in various journals till date are from the usage of the auto-correlation technique through schemes, like Knox-Thomson algorithm [20], shift and add [21], triple correlation [22], and Blind Iterative deconvolution (BID) technique [23] restore the degraded images. All these schemes, barring BID, depend on the statistical treatment of a large number of images. Often, it may not be possible to record a large number of images within the time interval over which the statistics of the atmospheric turbulence remains stationary. In such cases, where only a few images are available, we describe an auto-correlation algorithm that is developed under IRAF; this algorithm has been applied on degraded images of several binaries, obtained at the 2.34 m VBT at Kavalur.

## 2. Outline of the theory of speckle interferometry

The instantaneous image intensity distribution  $I(\mathbf{x})$  recorded by the detector (CCD/photographic plate/eye etc.) is actually a convolution of the instantaneous ‘Point Spread Function (PSF)’  $S(\mathbf{x})$ , with the actual intensity distribution of the object  $O(\mathbf{x})$ . Here  $\mathbf{x}$  is the two dimensional position vector. The PSF describes how light from a point source (a two dimensional  $\delta$  function on the sky) gets distributed across the detector. The variability of the corrugated wavefront yields ‘speckle boiling’ and is the source of speckle noise that arises from difference in registration between evolving speckle pattern and the boundary of the PSF area in the focal plane. These specklegrams have additive noise contamination,  $N(\mathbf{x})$ , which includes all additive measurement of uncertainties. This may be in the form of (i) photon statistics noise, and (ii) all distortions from the idealized isoplanatic model represented by the convolution of  $O(\mathbf{x})$  with  $S(\mathbf{x})$  that includes non-linear geometrical distortions.

If instead of dealing in the real space we choose to work in Fourier space, our life becomes simpler. This is because the operation of convolution in real space becomes simple multiplication in the Fourier space. Mathematically speaking:

$$I(\mathbf{x}) = O(\mathbf{x}) * S(\mathbf{x}) + N(\mathbf{x}), \quad (1)$$

where ‘\*’ signifies convolution operation.

In *Fourier* domain, equation (1) can be written as:

$$I(\mathbf{u}) = O(\mathbf{u}) \cdot S(\mathbf{u}) + N(\mathbf{u}), \quad (2)$$

where  $\mathbf{u}$  is the two dimensional spatial frequency vector and ‘.’ implies the ordinary operation of multiplication. The quantity  $O(\mathbf{u})$  is called the *Object Spectrum*, and  $S(\mathbf{u})$  the *Transfer function*.

If the exposure time is short enough then the atmosphere can be taken to be static during the exposure. The common term that describes this is that ‘the atmosphere has been *frozen* during the exposure’. From experiments it has been found that for exposures below 20 ms the atmosphere can be considered as fairly static for reasonably stable nights.

A large number of such short exposure images (specklegrams) of the object of interest is taken. Also images of a reference star which is known to be a unresolved star (i.e., a point source, a two dimensional  $\delta$  function on the sky) and which lies in the same isoplanatic patch as that of the program star, is taken at the same time. It is assumed that the atmospheric distortion affects the reference star in the same way as it does to the program star.

The ensemble average of the power spectrum is given by

$$\langle |I(\mathbf{u})|^2 \rangle = \langle |O(\mathbf{u})|^2 \rangle \cdot \langle |S(\mathbf{u})|^2 \rangle + \langle |N(\mathbf{u})|^2 \rangle. \quad (3)$$

The reference star being a single star, the Fourier transform of its image is unity, i.e.,  $O_{ref}(\mathbf{u}) = 1$ .

The power spectrum of the program star is therefore given by

$$|O_{pro}(\mathbf{u})|^2 = \frac{\langle |I_{pro}(\mathbf{u})|^2 \rangle}{\langle |I_{ref}(\mathbf{u})|^2 \rangle}, \quad (4)$$

and by Wiener-Kinchin theorem, the autocorrelation of the object is given by

$$A[O(\mathbf{x})] = \mathcal{FT}^{-1}[|O(\mathbf{u})|^2], \quad (5)$$

where  $A$  denotes Autocorrelation and  $\mathcal{FT}^{-1}$  denotes the operation of inverse Fourier transform.

### 3. Data Processing and Noise Reduction

The program for finding the power spectrum is written in FORTRAN. It uses IRAF commands and hence the macros in IRAF are called and used. The program is written in such a way that a large number of data files can be handled and large number of images can be averaged to increase the signal-to-noise ratio. The set of input specklegrams of object and the reference stars are read and their power spectrum is calculated. The object power spectrum and the image power spectrum are averaged in the Fourier space. Finally the autocorrelated image is calculated using another programme.

The disadvantage with a division as in equation (4), is that the zeros in the denominator will corrupt the ratio and spurious high frequency components will be created in the reconstructed image. Moreover, a certain amount of noise is inherent in any kind of observation. In our present case noise is primarily due to thermal electrons in the CCD interfering with the signal. Most of this noise is in the high spatial frequency regime.

In order to get rid of this high frequency noise as much as possible, a Wiener filter was used. Applying the Wiener filter is essentially the process of convolving the noise degraded image  $I(\mathbf{x})$  with the Wiener filter. The Wiener filter is applied in the frequency domain. Then the original image spectrum  $I(\mathbf{u})$  is estimated from the degraded image spectrum  $I'(\mathbf{u})$  by simply multiplying the image spectrum with the Wiener filter  $W(\mathbf{u})$ . However, this will reduce the resolution in the reconstructed image. The advantage is the spurious higher frequency contribution are eliminated.

$$I(\mathbf{u}) = I'(\mathbf{u}) \cdot W(\mathbf{u}). \quad (6)$$

The Wiener filter, in the frequency domain, has the following functional form:

$$W(\mathbf{u}) = \frac{H^*(\mathbf{u})}{|H(\mathbf{u})|^2 + \frac{P_n(\mathbf{u})}{P_s(\mathbf{u})}}. \quad (7)$$

where,  $H(\mathbf{u})$  is the Fourier transform of the point-spread-function,  $P_s(\mathbf{u})$  the power spectrum of signal process, and  $P_n(\mathbf{u})$  the power spectrum of noise process.

The term  $P_n(\mathbf{u})/P_s(\mathbf{u})$  can be interpreted as reciprocal of signal to noise ratio. In our case, the noise is due to the CCD. We developed an IRAF-based algorithm, where a Wiener parameter,  $w$ , is added to the PSF power spectrum in order to avoid zeros in the PSF power spectrum that helps in reconstructions with a few frames. The classic Wiener filter that came out of the electronic information theory where diffraction-limits do not mean much, is meant to deal with signal dependent 'coloured' noise. In practice, this term is usually just a constant, a 'noise control parameter' whose scale is estimated from the noise power spectrum. In this case, it assumes that the noise is white and that one can estimate its scale in regions of the power spectrum where the signal is zero (outside the diffraction-limit for an imaging system). The expression for the Wiener filter simplifies to:

$$I(\mathbf{u}) = \frac{P_{ref}(\mathbf{u})}{P_{ref}(\mathbf{u}) + w}, \quad (8)$$

where,  $w$  is the noise-variance and termed as Wiener filter parameter in the program.

To get an optimally autocorrelated image, a judicious choice of the Wiener filter parameter is made according to the procedure described below:

For a very wide range of Wiener filter parameter values, the autocorrelated images are constructed. A small portion (16 X 16 pixels) of each image, far from the centre, is sampled to find-out the standard deviation in the intensity values of the pixels,  $\sigma_{noise}$ . The plot of standard deviation thus obtained against the Wiener filter parameter (Figures 1(c)) shows a minimum. The abscissa corresponding to this minimum gives the optimum Wiener filter parameter value.

The nature of  $\sigma_{noise}$  vs. WFP plot is understood as follows:

The noise in our data is primarily in the high frequency region whereas the signal is at a comparatively low frequency. With zero WFP, there is no filtering and hence there is ample noise. As the WFP value is gradually increased from zero, more and more high frequency noise is cut off and the  $\sigma_{noise}$  goes down. It attains a minimum when WFP value is just enough to retain the signal and discard the higher frequency noise. However, at higher WFP region, we are over compensating for the signal, and therefore blurring of the image starts to occur. This leads to the sharp increase in  $\sigma_{noise}$ . The ‘ringing’ effect due to sharp cutoff comes into play.

Computer simulations were carried out by convolving ideal star images having Gaussian profile with a random PSF to generate speckle pattern. The plot of  $\sigma_{noise}$  vs. WFP also gives similar results though some of the major sources of noise, e.g., thermal noise due to electron motion in the CCD, effect due to cosmic rays on the frame, etc. were not incorporated in the simulation.

#### 4. Instrumentation

The 2.34 m VBT has two accessible foci for back end instrumentation – a prime focus (f/3.25 beam) and a Cassegrain focus (f/13 beam). The latter was used for the observations described in this paper. The Cassegrain focus has an image scale of 6.7 arcseconds per mm. This was further magnified using a microscope objective [24]. This enlarged image was recorded through a 5 nm filter centred at  $H\alpha$  using an EEV intensified CCD camera which provides a standard CCIR video output of the recorded scene. The interface between the intensifier screen and the CCD chip is a fibre-optic bundle which reduces the image size by a factor of 1.69. A DT-2851 frame grabber card digitises the video signal. This digitiser re samples the pixels of each row (385 CCD columns to 512 digitized samples) and introduces a net reduction in the row direction by a factor of 1.27. Finally an image-scale of 0.015 arcsecond per pixel is achieved. The frame grabber can store upto two images on its onboard memory. These images are then written onto the hard disc of a computer.

## 5. Results

The separations of HR4689 and HR5858, observed on 28 February 1997 were estimated using the procedure described above. The average seeing was around 1.5 arcsec. Figures 1a, 1b, 1c show the specklegrams of HR4689, minimum noise autocorrelated image of HR4689, and variation of noise with Wiener filter parameter respectively. The separation of HR4689 was found to be  $0.17 \pm 0.03$  arcseconds and that of HR5858 was  $0.23 \pm 0.03$  arcseconds. The separations observed are compatible with the values published in the CHARA catalogue [25].

## 6. Discussion and conclusions

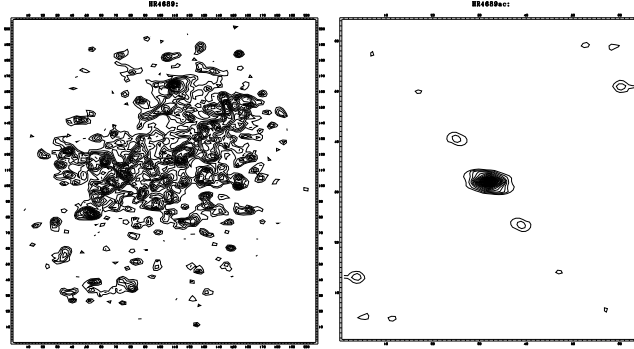
The program of speckle imaging of binary stars at VBT, Kavalur has been a successful one. Several experiments and computer simulations have been carried out for improving the speckle interferometer at VBT [3]. Algorithms are in stage of development for Fourier phase recovery too. Noise in the data is reduced to an optimum level with the judicious use of Wiener filter. Recent developments in CCD technology and associated photon counting devices of high quantum efficiency promise better signal to noise ratio, and hence better accuracy in determining the orbital parameters of binaries. However, in this algorithm, it gives a better signal to noise ratio if the reference star is brighter than the program star, both being in the same isoplanatic patch. This is very difficult to achieve in reality and when it is not fulfilled, we have tried to make a compensation by increasing the number of frames for the reference.

**Acknowledgments:** We would like to thank Mr. K. Sankarasubramanian for his constant help throughout the work, primarily in developing the algorithms and implementing them with success. The services rendered by Messrs V. Chinnappan, P. Anbazhagan, and V. Murthy are also gratefully acknowledged.

## References

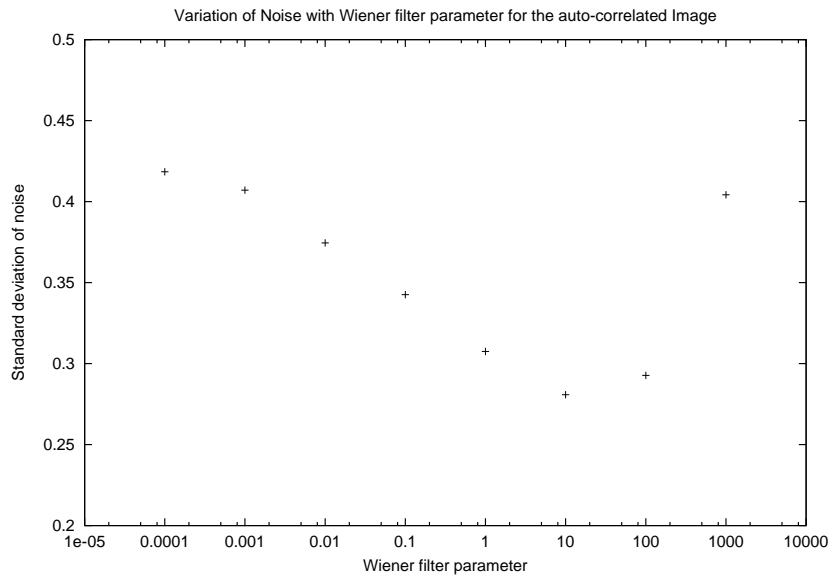
- [1] A. Labeyrie, 1970, *Astron. Astrophys.*, **6**, 85.
- [2] S. K. Saha, 1999a, *Bull. Astron. Soc. Ind.*, **27**, 443.
- [3] S. K. Saha, 1999b, *Ind. J. Phys.*, **73B**, 553.
- [4] H. A., McAlister, 1988, *Proc. ESO-NOAO conf. 'High Resolution Imaging Interferometry'*, ed. F. Merkle, Garching bei München, FRG, 3.
- [5] G. Torres, R. P. Stefanik, and D. W. Latham, 1997, *Astrophys. J.*, **485**, 167.
- [6] W. I. Hartkopf, B. D. Mason, H. A. McAlister, N. H. Turner, D. J. Barry, G. Franz, and C. M. Prieto, 1996, *Astron. J.*, **111**, 936.
- [7] W. I. Hartkopf, H. A. McAlister, and B. D. Mason, 1997, *CHARA Contrib.*

- No. 4, ‘Third Catalog of Interferometric Measurements of Binary Stars’, W.I.
- [8] H. A. McAlister, W. I. Hartkopf, B. D. Mason, L. C. Roberts (Jr.), and M. M. Shara, 1996, *Astron. J.*, **112**, 1169.
- [9] B. D. Mason, D. R. Gies, W. I. Hartkopf, W. G. Bagnuolo (Jr.), T. ten Brummelaar, and H. A. McAlister, 1998, *Astron. J.*, **115**, 821.
- [10] D. Bonneau, Y. Balega, A. Blazit, R. Foy, F. Vakili, and J. L. Vidal, 1986, *Astron. Astrophys. Suppl.*, **65**, 27.
- [11] A. Blazit, D. Bonneau, and R. Foy, 1987, *Astron. Astrophys. Suppl.*, **71**, 57.
- [12] N. Miura, N. Baba, S. Isobe, M. Noguchi, and Y. Norimoto, 1992, *J. Modern Opt.*, **39**, 1137.
- [13] I. I. Balega, Y. Y. Balega, I. N. Belkin, A. E. Maximov, V. G. Orlov, E. A. Pluzhnik, Z. U. Shkhagosheva, and V. A. Vasyuk, 1994, *Astron. Astrophys. Suppl.*, **105**, 503.
- [14] E. P. Horch, Z. Ninkov, W. F. van Altena, R. D. Meyer, T. M. Girard, and J. G. Timothy, 1999, *Astron. J.*, **117**, 548.
- [15] G. G. Douglass, R. B. Hindsley, and C. E. Worley, 1997, *Astrophys. J. Suppl.*, **111**, 289.
- [16] C. Leinert, A. Richichi, and M. Haas, 1997, *Astron. Astrophys.*, **318**, 472.
- [17] S. K. Saha, and P. Venkatakrisnan, 1997, *Bull. Astron. Soc. Ind.*, **25**, 329.
- [18] M. E. Germain, G. G. Douglass, and C. E. Worley, 1999, *Astron. J.*, **117**, 1905.
- [19] S. K. Saha, R. Sridharan, and K. Sankarasubramanian, 1999a, ‘Speckle image reconstruction of binary stars’, Presented at the Astron. Soc. Ind. meeting, held at Bangalore, 1999.
- [20] Knox K.T. & Thompson B.J., 1974, *Ap.J. Lett.*, **193**, L45.
- [21] Lynds C.R., Worden S.P., Harvey J.W., 1976, *Ap.J.*, **207**, 174.
- [22] Lohmann A.W., Weigelt G., Wirtzner B., 1983, *Appl. Opt.*, **22**, 4028.
- [23] Ayers G.R. & Dainty J.C., 1988, *Optics Letters*, **13**, 547.
- [24] S. K. Saha, G. Sudheendra, A. Umesh Chandra, and V. Chinnappan, 1999b, *Experimental Astron.*, **9**, 39.
- [25] McAlister H. A. & Hartkopf W. I., 1988, CHARA contribution no. 2.



(a)

(b)



(c)

Figure 1: : 1a, 1b, 1c show the specklegram of HR4689, the autocorrelation of HR4689 and  $\sigma_{noise}$  vs. WFP plot respectively. The axes of the figures 1(a) and 1(b) are the pixel value; each pixel value is 0.015 arc-seconds. Since the inherent property of the autocorrelation method is to produce double images with  $180^\circ$  ambiguities of a binary source, one of the two contours on either side of the central one (fig 1b) is the secondary component; the central contours represents the primary component. The contours at the corners are the artifacts.